Available online at www.sciencedirect.com

SciVerse ScienceDirect

Advances in Space Research 49 (2012) 957–965

ADVANCES IN SPACE RESEARCH (a COSPAR publication)

www.elsevier.com/locate/asr

GNSS-R concept extended by a fine orbit tuning

J. Klokočník [a], A. Bezděk [a,*], J. Kostelecký [b,c]

[a] Astronomical Institute, Academy of Sciences of the Czech Republic, CZ-251 65 Ondřejov, Czech Republic
[b] CEDR – Research Institute for Geodesy, Topography and Cartography, CZ-250 66 Zdiby 98, Czech Republic
[c] Department of Advanced Geodesy, Czech Technical University, CZ-166 29 Praha 6, Thákurova 7, Czech Republic

Received 17 July 2011; received in revised form 11 November 2011; accepted 12 December 2011
Available online 17 December 2011

Abstract

Small changes in semimajor axis of the orbits selected for the GNSS-R [R as Reflectometry] satellites, so-called fine orbit tuning, known from the ESA's Gravity and steady-state Ocean Circulation Explorer mission, can dramatically increase the number of nadir and off-nadir reflecting points and, in turn, can enhance the capability of the concept of bistatic altimetry (GNSS Reflectometry) without additional costs. The application of our suggestion is feasible for a satellite which will be equipped by thrusters for the orbit keeping. During the mission lifetime several orbit tunings are feasible, just to transfer from one to another orbit. Then we can study short-periodic or longer-periodic features, according to scientific goals defined for the mission. The shortest cycles (few days), corresponding to the required revisit time (defined by ESA), may be subcycles of much longer cycles (repeat periods).

Keywords: Bistatic (GNSS-R) altimetry (reflectometry); PARIS concept; Orbit resonances; Fine orbit tuning

1. Introduction

Originally intended to extend possibilities of traditional, nadir, "monostatic" altimetry, the concept of bistatic altimetry – now called GNSS-R reflectometry – has many applications. It can be used as ordinary altimetry over the oceans and seas with much higher number of reflecting points (the off-nadir points), e.g. for early warning of severe weather conditions at sea (Unwin et al., 2003), for tsunami early-warning systems (Martín-Neira and Buck, 2005) or in geodynamics (Shum et al., in press). The refracted signals from the GNSS radio occultation satellites together with the ground GNSS observations may provide high-resolution tropospheric water vapour, temperature and pressure, tropopause parameters and ionospheric total electron content (Jin and Komjathy, 2010). For much more information about the GNSS-R concept and its progress, see *ESA GNSS-R 2010 workshop*, Barcelona, Spain, 21–22 October, 2010, or *2nd CNES CCT workshop on passive reflectometry using radiocom space signals, SPACE REFLECTO 2011*, Calais, France, 27–28 October, 2011.

The message of this article is very simple: we wish to present a strong argument for improving the utility of GNSS-R concept at little to no extra cost by simply tuning the orbital period to enhanced the ground track density (a detailed analysis like that for GOCE in Bezděk et al. (2010) would be too premature for the GNSS-R reflectometry satellites in the present-day situation of the project). First we outline the PARIS concept (Section 1.1), then we described orbital resonances and give necessary definitions in Section 1.2, we explain how the diagrams for evolution of resonances work (Section 1.3), giving some examples (Figs. 2, 3, 6 and 7), and we note on the orbit tuning for various satellites (Section 1.4) to optimize their orbits. Then it is already easy to apply the concept of the orbit tuning for the GNSS-R satellites (Section 2). Few examples are in Table 1. Still there are many options and before doing a possible detailed analysis we need to know more about the final orbit choice for those satellites. Then we will account also for the off-nadir points due to swaths of the

* Corresponding author.
E-mail addresses: jklokocn@asu.cas.cz (J. Klokočník), bezdek@asu.cas.cz (A. Bezděk), kost@fsv.cvut.cz (J. Kostelecký).

0273-1177/$36.00 © 2011 COSPAR. Published by Elsevier Ltd. All rights reserved.
doi:10.1016/j.asr.2011.12.008

Table 1
Density D [km] of the groundtracks and number N_x of the cross-over points for different repeat orbits, here $I > 90$ degrees.

	GOCE		GNSS-R					
Resonance	16:1	977:61	43:3	502:35	44:3	499:34	25:2	438:35
D [km]	2505	41	932	80	911	80	1603	92
N_x	256	1013149	1935	269072	2024	265468	650	206736

onboard GNSS-R antennae (we touched this topic already in Klokočník et al., 2005).

1.1. PARIS

The acronym PARIS means PAssive Reflectometry and Interferometry System, suggested and also patented by Martín-Neira (1993). Satellite antenna on the low Earth orbiting satellite is receiving signal from several GNSS satellites directly and also signal reflected from the ocean surface. The measured quantity is a delay between these two signals. Number of reflecting points may increase by multiples in a comparison with the traditional, nadir altimetry (it depends on limiting off-nadir angle, given by the swath, number of GNSS satellites used, etc.); thus, there is a great potential for a dense and fast (nearly) global coverage of data.

Thanks to technological progress, mainly the construction of special antennae, dedicated GNSS-R satellites could be launched and ESA considers a candidate in phase A now. It should be a *small demonstration satellite* piggybacked to another satellite for launch from a smaller launcher to sun-synchronous, retrograde, dawn-dusk orbit (6 am and 6 pm are times of equator crossings) at height 500–800 km. Later the *operational satellite* dedicated to GNSS-R concept should be launched again on the sun-synchronous orbit but at height 1300–1500 km (with slightly different orbit inclination than for the first satellite, but both sun-synchronous, which means the orbit inclination $I = 98$–101 degrees, where I depends mainly on height of flight). The intention is to have the *revisit time* (more in Section 1.2) about 4 days for the former and about 2 days for the latter mission. *Swath* is 900 km or 1500 km, respectively, and spatial resolution not worse than 10×100 km $\times$ km (D'Addio and Martín-Neira, 2010; Martín-Neira et al., 2011, Table 1).

Precise orbit determination of these satellites is not subject of this paper but it is crucial for the success of the whole project. The error budget in D'Addio and Martín-Neira (2010) counts with higher errors than in the case of traditional nadir altimetry (± 18 cm vs. few centimetres) but it is balanced by a significantly higher number of observations in GNSS-R. However, we need the GNSS-R orbits with the same accuracy as those of GNSS satellites, which is in general about ± 5 cm for each orbit component. This is not a trivial task. We recall our analysis of contributing errors in Wagner and Klokočník (2003) and namely in Kostelecký et al. (2005) where we consider errors of measurements, errors in orbits of GNSS and low Earth satellites as well.

Today, ESA's navigation office can achieve the accuracy about 1–3 cm in the radial direction and the 5–10 cm in the other components, for satellites on comparable orbits, equipped with GPS receivers (the information received by one of anonymous reviewers of our manuscript).

1.2. Orbit resonance and other definitions

The *orbital resonance* of the Earth artificial satellite is identified by the ratio $\beta{:}\alpha$, for an orbit having a groundtrack repeat rate of β nodal revolutions (each from a node of the orbit to the next one of the same type) over α nodal days (sidereal days with respect to the precessing orbit plane). These integers are co-prime, i.e. the ratio $\beta{:}\alpha$ must be irreducible, and define the fundamental resonance, but overtone and sideband resonances may also be relevant: the $\gamma - 1$th overtone is specified as $\gamma\beta{:}\gamma\alpha$, $\gamma = 1, 2, 3, \ldots$ with $\gamma\beta = m$, which is the order of the basic resonance (Gooding and King-Hele, 1989); a sideband resonance involves a fourth index, q, related to eccentricity. Here we assume effectively circular orbits. Note that for the sun-synchronous orbit the nodal day equals 86,400 sec.

Geometrically, exact resonance of a satellite orbit means commensurability such that the satellite returns above the same Earth's sub-satellite point after its β nodal revolutions around the Earth during α nodal days, after which the ground tracks would repeat. In reality, the orbit is affected by atmospheric drag and other perturbations, so exact resonance is an instantaneous state; we say the satellite passes through a $\beta{:}\alpha$ resonance.

In remote sensing, people speak about "repeatability" *($\beta{:}\alpha$)*, "repeat" or "repetition" period (α) [nodal days], and Exact Repeat Mission, ERM = resonant orbits of altimetry satellites for oceanography. We will use terminology from celestial mechanics as mentioned above.

Subcycle. In literature there are different meanings of this term. Let us consider $\beta{:}\alpha$ resonance with the repeat period α days. Each resonance $\beta_r{:}\alpha_r$ with $\alpha_r < \alpha$ and with a semimajor axis very close to semimajor axis corresponding to the $\beta{:}\alpha$ resonance yields a subcycle to the cycle α. In practice the difference in semimajor axes can be few tens of meters or few kilometres, it depends on the individual application and technical equipment (see also the term "dead-band" below). For our discussion here it is sufficient to place no other condition on α_r, β_r other than that they define a global groundtrack grid very close to that of $\beta{:}\alpha$ (but not so dense) and that they have no common divisors (cf. with Pie, 2008 or Rees, 1999).

The term *revisit time* means the time elapsed between two successive observations of a particular location on the Earth surface. For the nadir points, the revisit time equals the repeat period (or its part for a very close subcycle); when accounting for a swath, the revisit time becomes shorter. In this paper we work only with the repeat period. Swath will help us to fulfil very short revisit time required by ESA (2–4 days), Section 1.1. One can find such orbits where the revisit times correspond to the shortest subcycles of the cycles corresponding to the repeat period.

Fig. 1(a) shows the groundtrack patterns for the ERS 1 (European Remote Sensing) satellite, having reached its "commissioning orbit phase" of the 43:3 resonance after three nodal days. Fig. 1(b) is for the orbit only by a few kilometres lower, at the 502:35 resonance. The network of the ground tracks of this "one-month" repeat orbit creates (is "laid-down" on the Earth's surface) slowly (the complete coverage is achieved during 35 instead of 3 days), but is much finer (in other words, the density of the ground tracks and therefore the density of the nadir measurements is much higher) than for the 3-day orbit; it was so-called "oceanographic" or "multi-disciplinary" phase of ERS-1 ERM, followed then by a free-falling "geodetic" orbit (GM = geodetic mission in contrast to the ERM). More on the choice of orbits for altimetry missions, see, e.g. Parke et al. (1987). The 502:35 repeat orbit has a sub-cycle of 3 days (Fig. 2). So each 3 days a very similar groundtrack pattern as shown by Fig. 1(a) is obtained, but the orbit is not perfectly closed during those 3 days, while for the 43:3 it closes completely.

A satellite's passage through an orbit resonance was used to evaluate lumped geopotential harmonics (linear combinations of the harmonic geopotential coefficients of the relevant orders), see Gooding (1971), Klokočník (1976) and Gooding and King-Hele (1989), but in this paper we are not interested in the gravity field studies. The phenomenon of resonance will be used in another way and for another purpose.

The *density of the ground tracks at the equator*: it is defined as $D = o/\beta$, where the circumference $o = 40\,075$ km (for the Earth). In this definition we consider only one portion of the orbit, ascending or descending one. The quantity D can also be understood as the longitudinal spacing of adjacent satellite tracks at the equator.

Crossover (point) is a intersection point on the projection of the satellite orbit on the ground between the ascending and descending orbital tracks. *Number of crossover points* (crossovers) for one orbit (single-satellite crossovers) among the ascending and descending tracks is given by

$$N_x = \beta(\beta - u\alpha - 1) \tag{1}$$

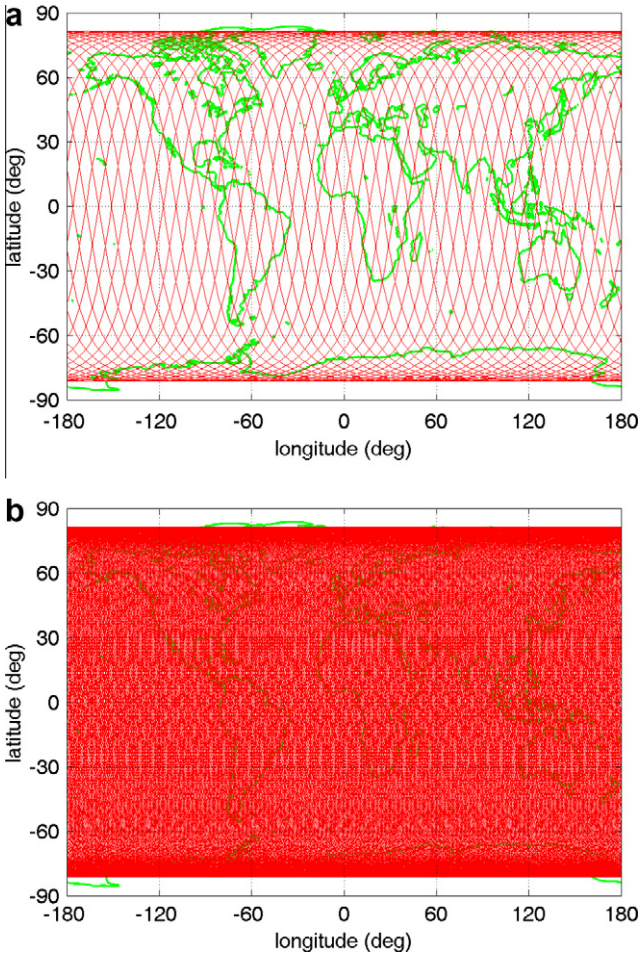

Fig. 1. (a) and (b). Grid of groundtracks for ERS 1 satellite. Panel 1 shows the groundtrack patterns of ERS 1 at the exact 43:3 resonances (no drag effect considered), after completing three nodal days. Altitude 775.1 km, inclination $I = 98.54$ degrees. Panel 2 shows the groundtrack patterns of ERS 1 at the exact 502:35 resonances (no drag effect considered), after completing 35 nodal days. Altitude 771.9 km, inclination $I = 98.54$ degrees.

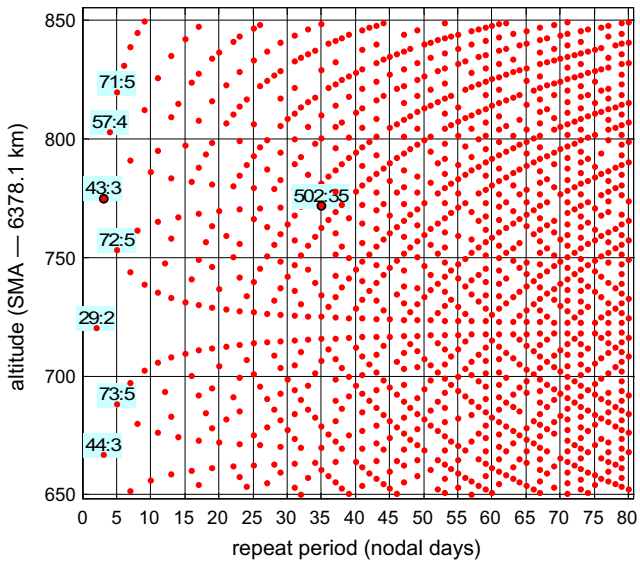

Fig. 2. Resonant diagram for ERS 1 ($I = 98.54$ degrees) with two different types of mean semimajor axis. First, at the commissioning phase of its flight the satellite was kept at the 43:3 resonance, then the orbit was manoeuvred to a bit lower 502:35 resonance for oceanographic applications (kept in the given orbit with about 1 km wide windows in altitude), and finally it was free-falling for geodetic applications (study of detailed marine geoid from altimeter measurements).

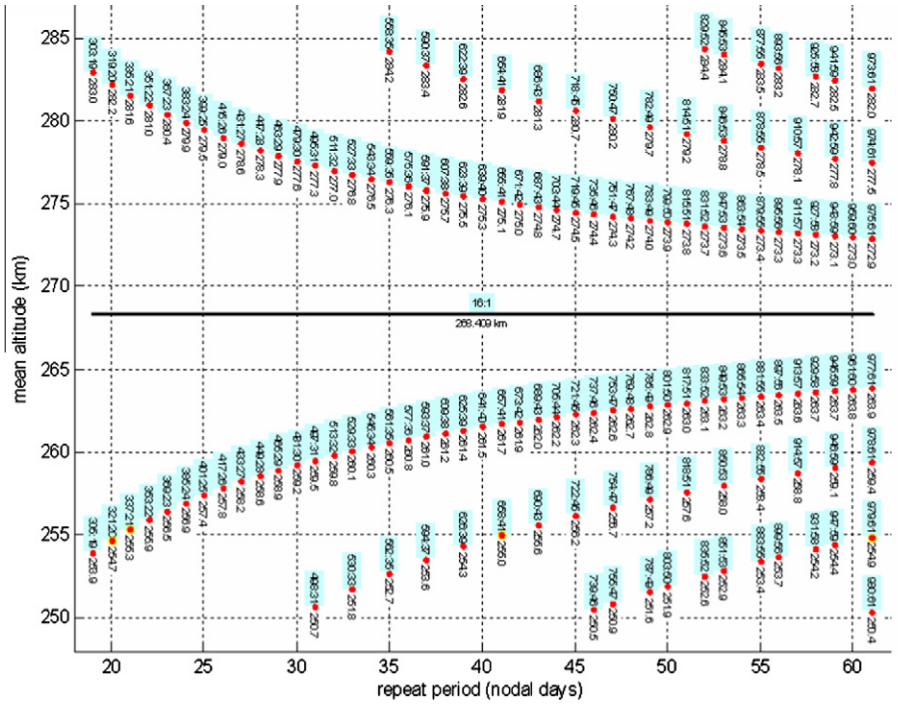

Fig. 3. Evolution of resonances for hypothetical free-fall of GOCE ($I = 96.7$ degrees). This diagram is used to select specific high-order resonant orbit. Ion motor on board of GOCE can keep altitude with about 10-meter precision.

where $u = 1$ for $I < 90$ and $u = -1$ for $I > 90$ degrees (e.g. Farless, 1986; Kim, 1997).

Dead-band concept. If the satellite is equipped with a propulsion system, the ground tracks can be maintained with a height tolerance ±X km dead-band. For older altimetry missions, it was about ±1 km. For GOCE, equipped by a fine ion motor, it was fantastic ±20 m at the beginning of the mission (2009) and now it is about ±5 m (Floberghagen, priv. commun. 2011). For GNSS-R, the value is not yet known but one can expect few hundred meters to one kilometre. Then, high order resonances with long repeat periods can mutually be closer (measured in height of the flight) than is the dead-band. This fact should be accounted for in forthcoming studies.

1.3. Diagrams for evolution of resonances

For the exact resonance β:α the following relationship between satellite mean (daily) motion n, semimajor axis a and inclination I can be found (Klokočník et al., 2008; Bezděk et al., 2009):

$$n = \frac{\beta}{\alpha}|\dot{S}|\left\{1 - \frac{3}{2}J_2\left(\frac{R}{a}\right)^2\left(4\cos^2 I - \tau\frac{\beta}{\alpha}\cos I - 1\right)\right\}, \qquad (2)$$

$J_2 = -\sqrt{5}\overline{C}_{20}, \dot{S} > 0$ for $\tau = 1$, and $\dot{S} < 0$ for $\tau = -1$, the former case for the normal rotation, the latter for the retrograde rotation (e.g. for Venus in the case of planetary orbiters) (Klokočník et al., 2010). In (2), R is radius of the Earth, $\dot{S}$ is its rotational speed, and $\overline{C}_{20}$ is dynamical flattening of the Earth. We will not deal with the details how to compute a from n and which type of a it should be (e.g. Kozai's, Brouwer's, t-averaged, or others – for a detailed explanation, see Klokočník et al. 2003). Our "height" is based on the mean semimajor axis of Brouwer's type and we have verified that this is the same that was used for GOCE (Floberghagen, priv. commun. 2009).

Now, using (2), we can understand the "resonance evolution diagrams" in Figs. 2, 3, 6 and 7. On the x-axis we have the repeat period of α nodal days, on the y-axis there is the mean semimajor axis, each graph point corresponds to a resonance and is labelled with the number β of the satellite nodal revolutions. These graphs are valid only for the particular inclination and selected range of semimajor axes. The results are valid for effectively circular orbits.

As time passes, the semimajor axis of the Earth's satellite contracts due to the atmospheric drag and the satellite orbit undergoes the resonances from top to bottom of the resonance evolution pictures. Obviously at each instant we can find a high order resonance (large β and relevant β:α), which however has no practical meaning from the view of study of the gravitational field, nor from viewpoint of oceanographic applications.

1.4. Note on the fine orbit tuning for gravity field missions

Orbit tuning to achieve an orbit most suitable for specific altimeter application is nothing new; it is known since ERS 1 (e.g., Reigber et al., 1988; Lefebvre and Vincent, 1988), see Figs. 1a and b and 2. It is a part of coverage analysis for various missions. Later it was discovered that

satellite-to-satellite tracking between GRACE A and B satellites, used to determine the monthly solutions for the geopotential and thus the time variations of it (Tapley et al., 2004; Bettadpur, 2006; Bruinsma et al., 2010, and others), which lost their accuracy when GRACE was at low-order resonance as was the 61:4 resonance in fall 2004. It was decoded that the lower accuracy of the results from measurements on/from a satellite is directly proportional to lower density of the ground tracks and that this is dictated by the order β of resonance. We can have the same quality and amount of satellite observations for the gravity field determination but their spatial distribution (in latitude and in longitude) is much poorer at a low order resonance (compare Fig. 1a–b, or Fig. 4a–b). This is that simple reason for a lower accuracy of the gravity field products. Note that the phenomenon of the accuracy decrease is only temporary; due to the atmospheric drag the semimajor axis (height of flight) of the satellite is steadily decreasing, thus the density of the ground tracks is changing with time. But we can change this situation by orbit keeping, see the case of GOCE.

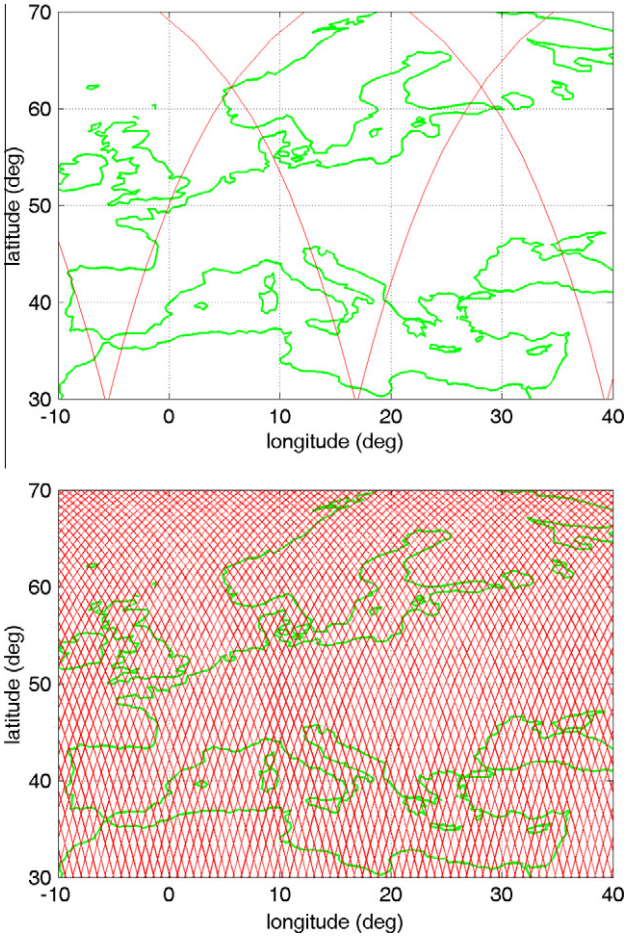

Fig. 4. Grid of groundtracks for GOCE satellite. The groundtrack densities at the 16:1 (upper panel) and 977:61 (lower panel) resonances of GOCE, zoomed to Europe, to better show the difference, compare the value of density D in Table 1. Altitude 268.4 km, $I = 96.7$ degrees in the upper panel, altitude 263.9 km, $I = 96.7$ degrees for the bottom panel.

There was a great inspiration from GRACE to GOCE. The satellite GOCE (Gravity field and steady-state Ocean Circulation Explorer, ESA) was launched in spring 2009 and is still working on an extremely low circular nearly polar orbit. For the first time it is equipped by a space gradiometer able to measure the full Marussi tensor (of the second derivatives of the disturbing gravitational potential) with the accuracy better than 1 milliEötvös [$1\text{E} = 10^{-9}\ \text{s}^{-2}$]. From GRACE we learned how to choose the appropriate orbit for GOCE by making small changes to its semimajor axis, these changes being known as "*fine orbit tuning*". This activity should avoid decrease in the accuracy of the gravity field products generated from the gradiometer measurements (compare theoretical case 16:1 to 977:61, Fig. 4). Nothing like temporary accuracy decreases in free-falling orbits of GRACE A/B should exist here if all systems on GOCE work as they should. The graphs based on (2) are basic tool for our estimates, but we have developed also more advanced numerical tools.

In Bezděk et al. (2009), we studied suitable repeat cycles in the vicinity (above and below) of the 16:1 resonance. We found that they differ greatly in stability towards small perturbations of the satellite's mean altitude and in the temporal evolution of the ground track coverage. Detailed analyses about the relationship of the low order resonances, ground track density changes and the accuracy of the gravity field parameters derived from such orbits have been published in Klokočník et al. (2008) and Weigelt et al. (2009). Similar analyses will also be needed for the GNSS-R satellite with the orbit keeping.

2. Proposal for GNSS-R satellites

The basic motivation for bistatic altimetry was to increase the number of reflecting points within a reasonable swath, in a comparison with the number of nadir/subsatellite points, to densify coverage by the measurements and not to lose (too much) precision. The GNSS-R concept was fully successful in this respect. The next step means further significant densification of the ground track network of reflecting points, mostly off-nadir.

2.1. Idea

Now we suggest to select the orbit by the fine orbit tuning (which means changes of the height by a few hundred meters or a few kilometres up or down) in such a way that it will be far from any low order resonance and – assuming that we have technical tool to keep the orbit in selected height for some time – to put and keep the satellite in one of many high order resonant orbits with α as long as useful (for a given application) and technically feasible, say 1 month. Then, the density of ground tracks D and the number of crossover points N_x will increase dramatically (theoretically by orders) in a comparison with the closest (in sense of semimajor axis or height of flight) low order resonant orbit. We have to tame our optimism,

however, because these are only theoretical considerations and the inclination of GNSS satellites $I \sim 65$ degrees (in a contrast to sun-synchronous orbits of GNSS-R satellites) will decrease the theoretical estimates roughly by 30–40%.

Another factor to be accounted for is that ESA requires very short revisit time, 2–4 days, to have chance to observe quickly fast features (even without a global coverage). But ESA also counts with the swath 650–1500 km (Section 1.1), which is helpful for the orbit tuning. Swath can be of comparable size or larger than D even for orbits with relatively low α. Although we cannot recommend resonant orbits of 2–4 days because of too low density D, we can select few orbits with the shortest subcycles a few days long, having much longer repeat periods α, say one month, to use the orbit (nearly ERM) also for monitoring of long-term features.

2.2. Possible practical application

To obtain the resonant evolution graphs for the sun-synchronous orbits, we combined (2) with the sun-synchronicity condition (Fig. 5). The resonant diagrams for the GNSS-R demonstration satellite in the height interval of 450–850 km is in Fig. 6(a) and the resonant diagram for the GNSS-R operation satellite planned to fly higher at 1250–1550 km is in Fig. 6(b). The lowest order resonance are the 15:1, 29:2, 43:3, and 44:3 in the former case and the 13:1 and 25:2 in the latter. Then we generated a zoom for a close vicinity of the 43:3 (height around 775 km), Fig. 7(a), at 44:3 (height around 666 km), Fig. 7(b), and of 25:2 (~1460 km), Fig. 7(c), as possible choices of low order three or two day revisit time orbits mentioned by D'Addio and Martín-Neira (2010). Then we selected two orbits below the orbits in the 43:3, 44:3, and 25:2 resonances, we computed the relevant D and N_x and prepared Table 1 (first columns are for the 16:1 and 977:61 resonances of GOCE). The "distance" of the selected orbits for the fine orbit tuning, counted from the nearest lower order resonance, is a few kilometres (Figs. 7(a)–(c)).

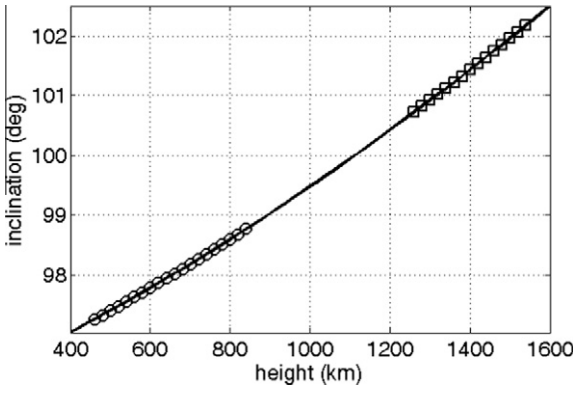

Fig. 5. Graph relating the height and inclination for a sun-synchronous circular orbit. It is derived from the secular motion of the ascending node, which has to be equal to the annual motion of the Earth around the Sun (see e.g. Montenbruck and Gill, 2001, p. 50). Highlighted are the orbital configurations corresponding to the first, GNSS-R "demonstration" satellite (450–850 km; circles) and to the second, GNSS-R "operation" satellite (1250–1550 km; rectangles).

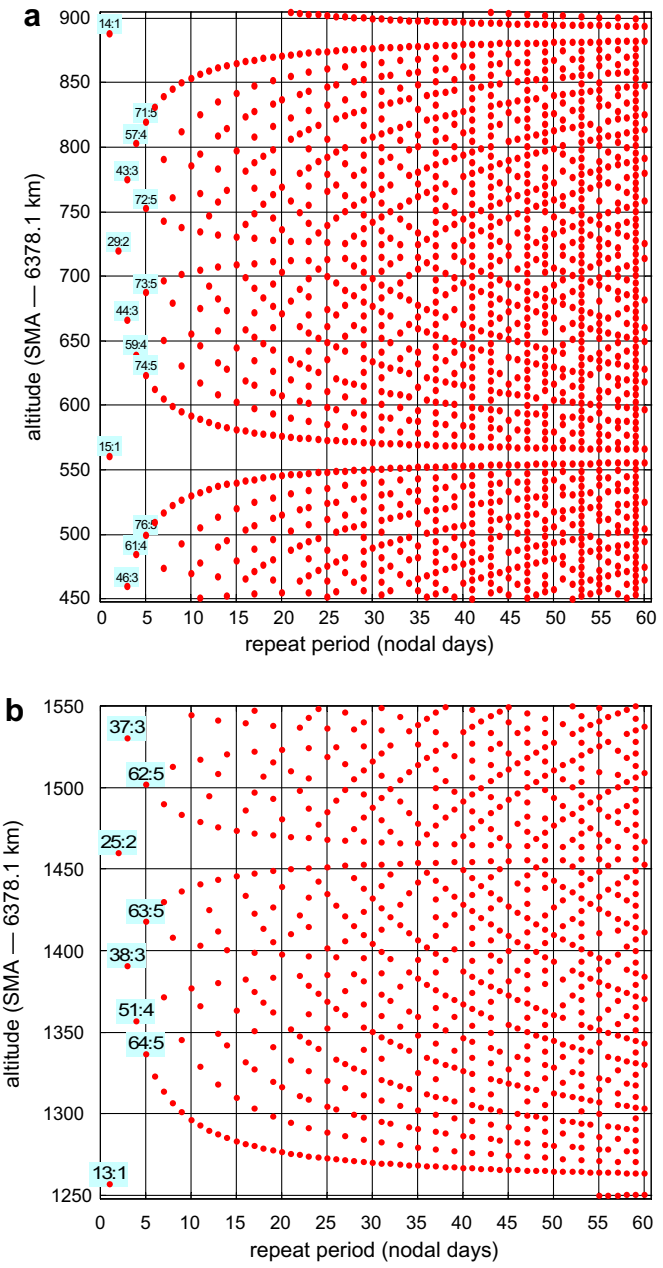

Fig. 6. (a) and (b) Graphs of resonances for sun-synchronous orbits in the height range: 450–850 km (Fig. 6(a), upper panel) and 1250–1550 km (Fig. 6(b)). The relevant inclinations are 97.2–98.8 degrees and 100.7–102.2 degrees, respectively.

The orbit selection, fine tuning and keeping has four conditions:

1. To select the orbit off any low order resonance (2–4 days resonances). The groundtrack density might be too low. But see also item 4.
2. To select the orbit below them (for the case that the orbit keeping does not work and the orbit above a low order resonance would pass through it).

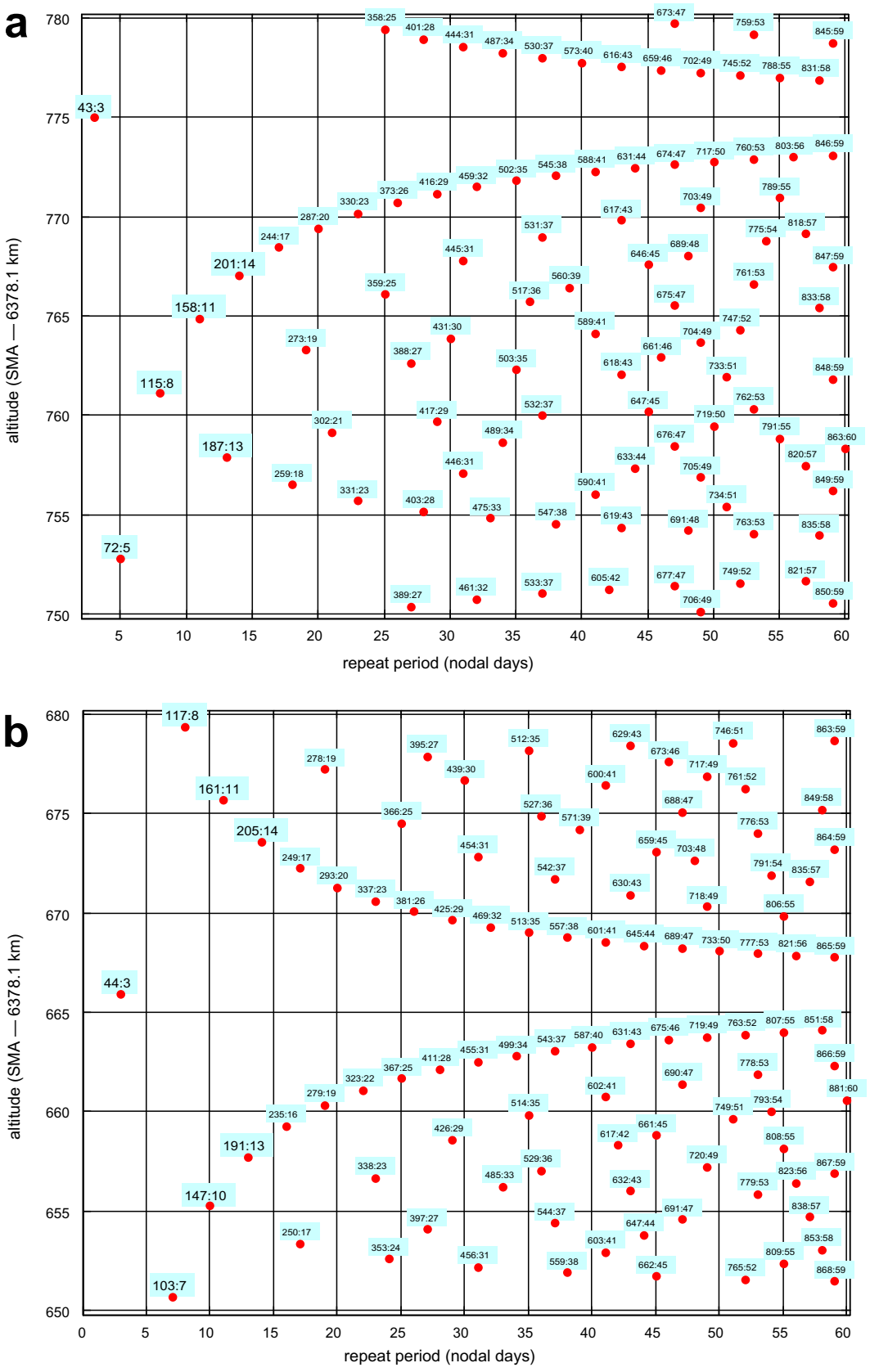

Fig. 7. (a)–(c). Zoom of the resonance graphs in Figs. 6(a) and (b) in the vicinity of resonances 43:3 (Fig. 7(a), upper figure), 44:3 (Fig. 7(b)) and 25:2 (Fig. 7(c)). The orbit designer has many choices, for different altitudes and repeat period intervals. The shorter cycles may be the subcycles of the longer cycles. This is probably the best solution to consider such subcycles for the required very short revisit time (few days), accounting for large swaths, while the repeat period may be significantly longer (weeks). Then we would have significantly reduced number of orbit choices. Let us move only parallel with the x-axis in Fig. 7(c) (i.e. for a constant, selected altitude). We see that the "resonance boughs" nearest to the lowest order resonance (25:2 in Fig. 7(c)) have no subcycles, while the others have one, two, three, and more subcycles on the boughs further from the height of the 25:2 resonance, symmetrically up or down.

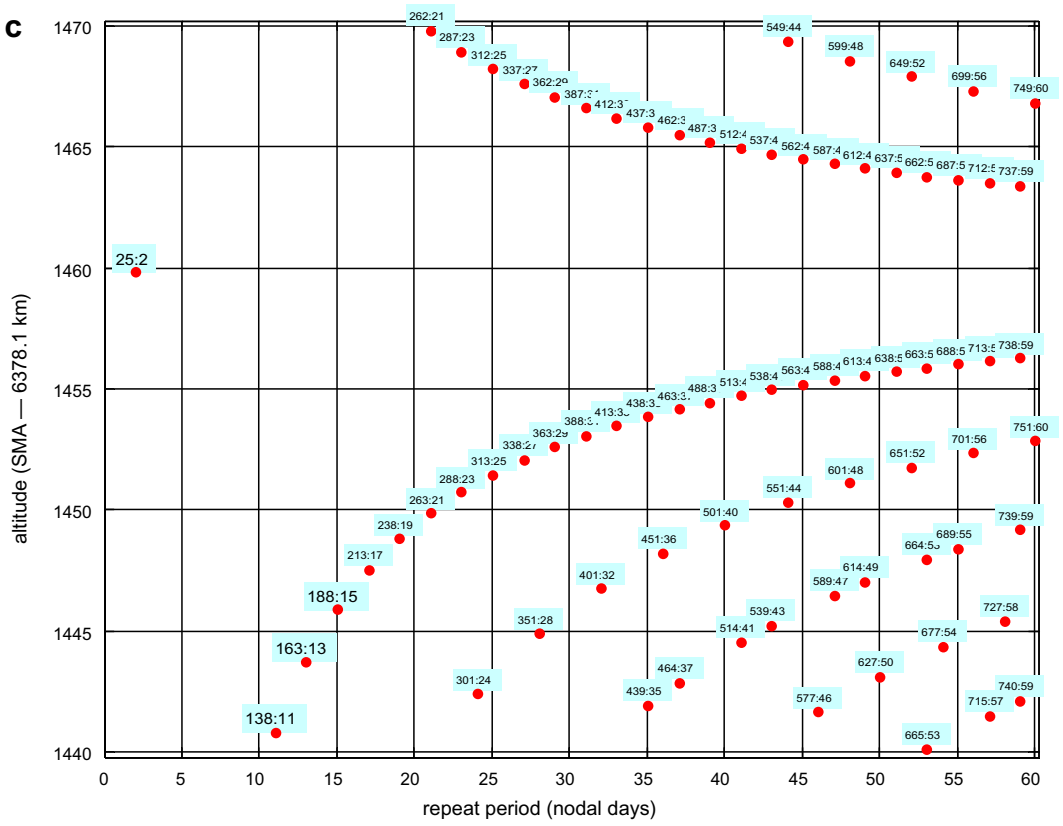

Fig 7. *(continued)*

3. To select the "best" β:α resonance on the appropriate "bough" of resonances properly. How high α will actually be, depends on technical possibilities and on parameters of the orbit keeping system on board.
4. But thanks to the swath we can select orbits *close* to low resonant orbits; those 2–4 days would then be the shortest subcycles, while the repeat period α can be much longer. For example, the demonstration mission may start its free-fall at the 57:4 resonance located at the altitude of 802.9 km, slightly below the 14:1 (Fig. 6(a)). The 57:4 resonance have neighbouring longer cycles, e.g. 841:59 or 442:31, of 1.4 km and 2.7 km respectively below the 57:4 orbit altitude. The operational satellite may be put near the 38:3 resonance at altitude 1390.8 km (Fig. 6b), having 3-day (the shortest) subcycle below the 25:2 resonance. The relevant one-month or two-month longer cycles closest to it (in semimajor axis) would be 393:31 (1386.4 km) and 735:58 (1388.4 km).

We have to say more about item 3. In Figs. 6 and 7, we see various branches of the "resonant tree", some without subcycles, some with them. On Fig. 7(a) for example, we can see the bough (branch) just below the 43:3 resonance that contains resonances … 244:17, 287:20, 330:23, etc … 846:59, etc. These orbits have no subcycles. The next bough below the previous one, with 617:43 among others, has one subcycle, i.e. 330:23. The branches below the previous have more and more subcycles. The evolution of the ground tracks for the resonant orbits without the subcycles differs remarkably from those with them. In the former case, the network of ground tracks evolves slowly, chronologically, but with a "final", higher density, while for the former case, faster but a lower density is created (during that subcycle or those subcycles), putting new groundtracks between already existing groundtracks created by the previous subcycle; for figures, see Bezděk et al. (2009). The result, as for the density and the geometry of the groundtracks, after the whole repeat period α, is the same.

The "orbit designer" had many choices. With conditions 1–4, the freedom of choice may become very limited. During the mission lifetime several orbit tunings are feasible, just to transfer from one to another orbit. Then we can study short-periodic features, with short α, later a long(er)-periodic features – our examples here are with α to about one month. The shorter cycles may be subcycles of the longer cycles. This is probably the best solution to consider such subcycles for the required very short revisit time (few days), accounting for large swaths, while the repeat period may be significantly longer (weeks).

3. Preliminary conclusions

The message of this paper is that a part of the proper orbit selection or orbit optimization, namely so-called fine

tuning in semimajor axis, can enhance the capability of the measured results from the GNSS-R as for their amount, coverage and precision without any additional costs for the orbit keeping. The fine orbit tuning, accounting for the required short revisit time (few days) as subcycles of much longer cycles – repeat periods (weeks), and also accounting for large swaths with many off-nadir measuring points, will be studied in near future in close cooperation with ESA.

Acknowledgments

This work has been supported by grant ESA PECS C 98056. We are grateful for discussions with Drs. Manuel Martín-Neira, Berthyl Duesmann (ESTEC ESA), and Carl A. Wagner (NOAA). We also acknowledge one of the reviewers for the constructive comments leading to an improvement of our manuscript.

References

Bezděk, A., Klokočník, J., Kostelecký, J., Floberghagen, R., Gruber, C. Simulation of free fall and resonances in the GOCE mission. J. Geodyn. 48, 47–53, doi:10.1016/j.jog.2009.01.007, 2009.

Bezděk A., Klokočník J., Kostelecký J., Floberghagen R., Sebera J., Some aspects of the orbit selection for the measurement phases of GOCE, in: Proc. of the ESA Living Planet Symposium, Bergen, Norway, ESA SP-686, 28 June–2 July 2010.

Bettadpur, S. Status of re-processed GRACE gravity field data products, EGU Vienna. Geophys. Res. Abstracts 8, 01563, 2006.

Bruinsma, S., Lemoine, J.-M., Biancale, R., Valès, N. 10-day gravity field models (release 2) and their evaluation. Adv. Space Res. 45, 587–601, doi:10.1016/j.asr.2009.10.012, 2010.

D'Addio, S., Martín-Neira, M., Observation of a PARIS altimeter in-orbit demonstrator in: Presenetd at ESA GNSS-R 2010 workshop, Barcelona, Spain, 21–22 October 2010.

Farless, D.L. The application of periodic orbits to TOPEX mission design, in Astrodynamics 1985, vol. 58, Part I "Advances in the Astronaut. Sci., in: Proc. AAS/AIAA Astrodynamics Conference, Vail, Colorado, August 12–15, pp. 13–36, 1986.

Gooding, R.H. Lumped fifteenth-order harmonics in the geopotential. Nature Phys. Sci. 231, 168–169, 1971.

Gooding, R.H., King-Hele, D.G. Explicit form of some functions arising in the analysis of resonant satellite orbits. Proc. R. Soc. Lond. A 422, 241–259, 1989.

Jin, S., Komjathy, A. GNSS reflectometry and remote sensing: New objectives and results. Adv. Space Res. 46, 111–117, doi:10.1016/j.asr.2010.01.014, 2010.

Kim, M.C. Theory of satellite ground-track crossovers. J. Geodesy 71, 749–767, 1997.

Klokočník, J. Changes in inclination of a close Earth satellites due to orbital resonances. Bull. Astronom. Insts. Cs 27, 287, 1976.

Klokočník, J., Kostelecký, J., Gooding, R.H. On fine orbit selection for particular geodetic and oceanographic missions involving passage through resonances. J. Geodesy 77, 30–40, doi:10.1007/s00190-002-0276-3, 2003.

Klokočník, J., Wagner, C.A., Kostelecký, J., Bezděk, A., Novák, P., McAdoo, D. Variations in the accuracy of gravity recovery due to ground track variability: GRACE, CHAMP, and GOCE. J. Geodesy 82, 917–927, doi:10.1007/s00190-008-0222-0, 2008.

Klokočník, J., Bezděk, A., Kostelecký, J., Sebera, J. Orbit tuning of planetary orbiters for accuracy gain in gravity-field mapping. J. Guidance, Control, Dyn. 33, 853–861, 2010.

Kostelecký, J., Klokocník, J., Wagner, C.A. Geometry and accuracy of reflecting points in bistatic satellite altimetry. J. Geodesy 79, 421–430, 2005.

Lefebvre, M., Vincent, R. An Orbit Scenario Fitting Most of Constraints of Altimeter, SAR, and Scaterometer Missions, ERS 1 Sampling Capabilities, French PAF for ERS-1, CNES Techn. Rep., Toulouse, 1988.

Martín-Neira, M. A passive reflectometry and interferometry system (PARIS) application to ocean altimetry. ESA J. 17, 331–355, 1993.

Martín-Neira, M., Buck, Ch. A tsunami early-warning system – the PARIS concept. ESA Bull 124, 50–55, 2005.

Martín-Neira, M. d'Addio, S., Buck, C., Strauch, K., Karafolas, N., Alcazar, J., Vitulli, R. PARIS In-Orbit Demonstration Mission in: Presented at workshop 'Advanced RF Sensors and Remote Sensing Instruments', 13–15 September ESA/ESTEC, Noordwijk, The Netherlands, 2011.

Montenbruck, O., Gill E. Satellite orbits – Models, methods and applications, Springer, Corrected 2nd Printing, ISBN 3-540-67280-X, 2001.

Pie, N. Mission design concepts for repeat groundtrack orbits and application to the ICESat mission. PhD dissertation thesis, University of Texas at Austin, USA, 2008.

Parke, M.E., Steward, R.H., Farless, D.L. On the choice of orbits for an altimeter satellite to study ocean circulation and tides. J. Geophys. Res. 92 (C11), 11693–11708, doi:10.1029/JC092iC11p11693, 1987.

Reigber, Ch., Klokočník, J., Li, H., and Flechtner, F. Contribution to ERS-1, Orbit Dossier, German PAF for ERS-1, DGFI Rep. 1988, Munich, Germany, 1988.

Rees, G. The remote sensing data book. Cambridge University Press, ISBN 0 521 48040 X, 1999.

Shum, C.K., Lee, H., Abusali, P.A.M., Braun, A., Guy de Carufel, Fotopoulos, G., Komjathy, A., Kuo, Ch., Prospects of Global Navigation Satellite System (GNSS) reflectometry for geodynamic studies, Advances in Space Research, in press, 10.1016/j.asr.2010.07.026.

Tapley, B., Bettadpur, S., Watkins, M., Reigber, Ch. The gravity recovery and climate experiment: mission overview and early results. Geophys. Res. Lett. 31 (9), doi:10.1029/2004GL010020, 2004.

Unwin, M.J., Liddle, J.D., Jason, S.J. GPS/GNSS reflectometry nano-satellite demonstration mission. Phil. Trans. R. Soc. Lond. A 361, 41–43, 2003.

Wagner, C.A., Klokočník, J. The value of ocean reflections of GPS signals to enhance satellite altimetry: data distribution and error analysis. J. Geodesy 77, 128–138, doi:10.1007/s00190-002-0307-0, 2003.

Weigelt, M., Sideris, M.G., Sneeuw, N. On the influence of the ground tracks on the gravity field recovery from high-low satellite-to-satellite tracking missions: CHAMP monthly gravity field recovery using the energy balance approach revisited. J. Geodesy 83, 1131–1143, doi:10.1007/s00190-009-0330-5, 2009.